Available online at www.sciencedirect.com
SCIENCE DIRECT
Solid State Communications 137 (2006) 212–215
solid state communications
www.elsevier.com/locate/ssc

Synthesis of lanthanum nickelate perovskite nanotubes by using a template-inorganic precursor

Mario Tagliazucchi [a], Rodolfo D. Sanchez [b], Horacio E. Troiani [b], Ernesto J. Calvo [a,*]

[a] *INQUIMAE-DQIAyQF, Facultad de Ciencias Exactas y Naturales, Universidad de Buenos Aires, Buenos Aires, Argentina*
[b] *Centro Atómico Bariloche and Instituto Balseiro, UNC, CNEA, Av. Bustillo 9500, 8400 SC de Bariloche, RN, Argentina*

Received 13 July 2005; accepted 6 November 2005 by B.-F. Zhu
Available online 1 December 2005

Abstract

A new route to obtain metal oxide nanotubes is presented: an inorganic coordination complex precursor containing the metal ions and impregnated into alumina membrane templates yield hollow tubular nanostructures of $LaNiO_3$ by calcination at 600 °C as characterized by powder X-ray diffraction (XRD). Scanning electron microscopy (SEM) shows that the resulting nanotubes have 200 nm in diameter in good agreement with the template pore. Transmission electron microscopy (TEM) and dark field transmission electron microscopy (DF-TEM) show that the nanotubes with 10–20 nm walls and internal separations are composed of 3–5 nm crystals.

PACS: 81.05.Je; 81.07.De; 81.20.Ka

Keywords: A. Nanostructures; B. Nanofabrications; B. Precursor; C. Scanning and transmission electron microscopy

1. Introduction

Low dimensional nanostructured materials have attracted considerable scientific attention due to their unique properties and possible applications. In particular nanoparticles (NPs), nanowires (NWs) and nanotubes (NTs) of carbon [1], metals, oxides, semiconductors [2,3] and polymers have been reported. In these materials the nanostructure optimizes the surface/volume ratio, an essential feature in applications such as catalysis.

The synthesis of inorganic perovskite oxide tubular nanostructures has recently been reported [4–8] which widens the opportunities to improve the catalytic activity and the possibility of use in fuel cells [9]. The synthesis of rare-earth manganese oxide NTs with 800 nm external diameter has been reported recently using a pore wetting technique [4] as well as the hydrothermal synthesis of single-crystal $La_{0.5}Sr_{0.5}MnO_3$ nanowires [10] and single crystal nanocubes of $La_{1-x}Ba_xMnO_3$ [11]. $LaNiO_3$ is a perovskite with metal conductity and Pauli paramagnetism [12,13]. Note that in the homologous series of rare earth mixed oxides, $La_{n+1}Ni_nO_{3n+1}$ [14], $LaNiO_3$ contains nickel in the trivalent state while the tetragonal La_2NiO_4 phase is the lowest oxidized with Ni(II). Films of this La–Ni oxide prepared by different routes have found broad applications in electrocatalysis: i.e. in oxygen evolution and reduction [15], as anode in alkaline water electrolysis [16]. More recently, this material has also been applied in non-conventional Si electronics as a good candidate for metallic electrodes, due to its good metallic behavior at room temperature and the matching lattice parameters to deposit other ferroelectric perovskites [17,18], magnetoresistive manganites and superconductors with high critical temperature [19].

Several low temperature methods for the preparation of $LaNiO_3$ have been reported with advantages over the reaction of NiO and La_2O_3 in a molten carbonate flux at 800 °C [20]. These milder techniques include (i) decomposition of mixed oxalates [21], nitrates or carbonates [22], (ii) sol–gel [23], (iii) liquid-mix technique [24], (iv) decomposition of metalorganic [25,26] or metalo-inorganic precursors [27,28]. The synthesis of nanosized lanthanum nickel oxide powder has been reported by thermal decomposition (600–700 °C) of an amorphous La–Ni diethylene–triaminepentaacetic acid complex [29].

C.P. Tavares reported the preparation of $LaNiO_3$ by low temperature thermal decomposition of the inorganic precursor, $NH_4La[Ni(NO_2)_6]\cdot xH_2O$ [27]. The synthesis, characterization and thermal decomposition of nickel nitro complexes including

* Corresponding author. Tel.: +54 11 4576 3379; fax: +54 11 4576 3341.
E-mail address: calvo@qi.fcen.uba.ar (E.J. Calvo).

0038-1098/$ - see front matter © 2005 Elsevier Ltd. All rights reserved.
doi:10.1016/j.ssc.2005.11.022

the related $KLa[Ni(NO_2)_6]\cdot xH_2O$ that yields $LaNiO_3$ upon heating at 500–700 °C, has been recently reported [28].

In this communication, a new strategy is presented to obtain $LaNiO_3$ nanotubes by thermal decomposition of the soluble inorganic precursor $NH_4La[Ni(NO_2)_6]\cdot xH_2O$ impregnated into Al_2O_3 template nanopores. Relative low temperature decomposition yields the desired Ni(III) mixed oxide in an oxidizing environment with La and Ni distributed in the solid precursor at the nanometer scale, thus avoiding the slow inter-diffusion of ceramic methods. Dissolution of the Al_2O_3 membrane in alkali produces free standing $LaNiO_3$ NTs. It is suggested that the bigger the cation the easier is its incorporation in the nickel nitro complex crystalline structure; thus NH_4^+ with almost the same size of K^+ is expected to favor the formation of the desired precursor from a lanthanum nitrate solution containing excess ammonium ions.

Membrane template-directed synthesis has been employed to grow nanowires [30] and nanotubes [31] of a variety of materials such as metals, semiconductors [2,3], oxides, polymers, using alumina or polycarbonate membranes, with vertically oriented pore arrays. The combination of soluble $NH_4La[Ni(NO_2)_6]\cdot xH_2O$ with the desired metal atom ratio and the low temperature decomposition of the precursor filling the pores of the alumina template provides a unique new method for the synthesis of hollow oxide nanostructures with very small crystals forming the walls.

2. Experimental

For the synthesis of $NH_4LaNi(NO_3)_6\cdot xH_2O$; stoichiometric quantities of $La(NO_3)_3\cdot 6H_2O$, $Ni(NO_3)_3\cdot 6H_2O$ and NH_4NO_3 were dissolved in the minimum amount of warm water; $NaNO_2$ was dissolved in cold water to prevent nitrite decomposition and both solutions were mixed cooling in an ice-bath with continuous stirring. The resulting green solution was stored at 0 °C for 2 days and a light orange precipitate was collected. After filtering the precipitate, it was washed successively with ice-cold water and acetone and dried in air and afterwards it was further characterized by elemental analysis and FTIR.

In order to fill the pores of the hydrophilic alumina template, a saturated solution of the $NH_4La[Ni(NO_2)_6]\cdot xH_2O$ precursor was filtered through the Al_2O_3 membrane (Anapore® Whatman® of 60 μm thickness and nominal 200 nm pore diameter with 10^9 pores cm^{-2}) or filled by capillarity and the excess solution was removed from the membrane faces. After drying the membrane in oven at 60 °C for half an hour an orange color becomes apparent and after calcination at 600 °C for 24 h the ceramic template turns black. The membranes were dissolved in 2 M KOH and the free standing $LaNiO_3$ NTs were purified by three successive centrifugation–washing steps.

Fourier transform infrared spectra (FTIR) of the precursor complex was recorded in KBr pellet using a Nicolet 510P spectrometer provided with a DTGS detector and a Balston 75-45 purge gas generator. Thermogravimetry was performed on a Shimadzu TGA-51 instrument, under air flow. The XRD patterns were recorded with Siemens 5000 difractometer using Cu Kα1 radiation. SEM and TEM images were obtained with a SEM Phillips XL30 CP and with a Philips CM 200 TEM microscope equipped with and ultratwin objective lens and acceleration potential was 200 keV, respectively.

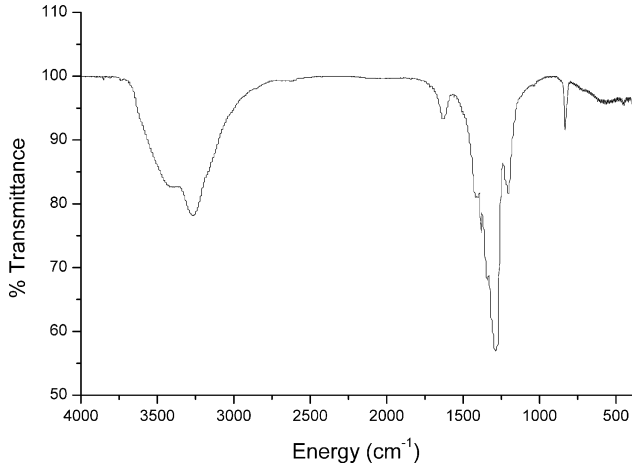

Fig. 1. FTIR spectra of $NH_4La[Ni(NO_2)_6]\cdot xH_2O$ in KBr pellet.

3. Results and discussion

Fig. 1 shows the infrared spectra of $NH_4LaNi(NO_3)_6\cdot xH_2O$. The four peaks in the region of 1200–1400 cm^{-1} could be assigned to the symmetric and anti-symmetric stretching of nitro and nitrite groups [32]; a band at 832 cm^{-1} could be assigned to ONO deformation and the broad band at 3200–3400 cm^{-1} is observed in the region where ammonium N–H and water O–H stretching modes are expected.

The elemental chemical analysis of the precursor showed always a small defect in lanthanum with respect to nickel probably due to contamination with $M_4[Ni(NO_3)_6]$ (where M = Na^+, NH_4^+) in spite of the expected preferential incorporation of large cations like La^{3+} and NH_4^+ in the crystalline structure [27]. This might cause sodium contamination, which unlike volatile ammonium remains trapped in the solid affecting the La:Ni ratio.

The thermogravimetry of $NH_4LaNi(NO_3)_6\cdot xH_2O$ precursor in Fig. 2 shows that the largest mass loss occurs at lower

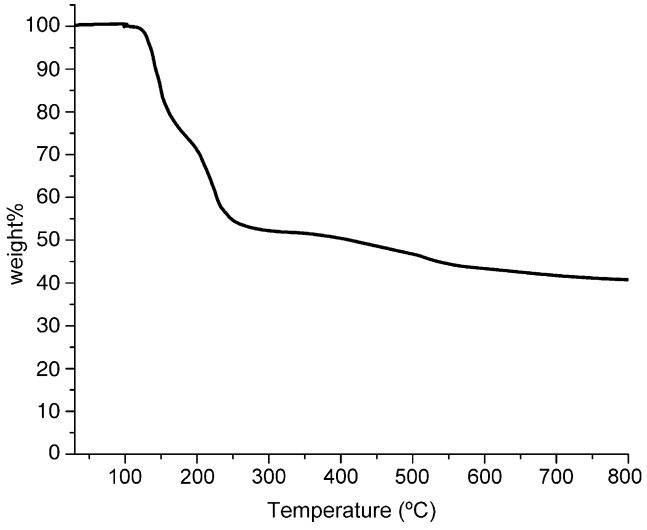

Fig. 2. Thermogravimetric (TGA) analysis of the $NH_4La[Ni(NO_2)_6]\cdot xH_2O$ precursor.

temperature than $K_4Ni(NO_2)_6$, ca. 100–150 °C [28], loosing water, ammonia and nitrogen oxides and continues up to 550–600 °C where the perovskite phase is obtained. The observed mass loss of 56.2% at 600 °C is in good agreement with a value of $x=4$ (calculated mass loss: 56.4%). Previous studies on related complexes [28] have shown a mass gain in air around 500 °C which was indentified as an oxidation reaction of nitrites. This gain was not observed for $NH_4La[Ni(NO_2)_6]$-xH_2O, probably due to fast decomposition of ammonium nitrite. It has also been observed that the ammonium solid complex is less stable than the potassium one decomposing in a few days.

In a series of related complexes of general formula $K_2M(Ni(NO_2)_6)$ with M = Ba, Pb and Sr, Takagi et al. [33] reported cubic structures. Based on these results, Bolibar et al. [28] indexed $KLa[Ni(NO_2)_6]$ as a cubic unit cell with lattice parameter 10.571 Å. Since, the ionic radius of K^+ and NH_4^+ are very similar, it is expected that our precursor $NH_4La[Ni(NO_2)_6]$ has similar lattice parameters. Therefore, the La–Ni and Ni–O distances in the precursor should be about 5.3 and 2.9 Å, respectively, close to the final values in the LaNiO3 perovskite, ca. 3.34 and 1.93, respectively. The La–Ni crystalline precursor avoids the need for long diffusion distances characteristic of ceramic methods.

Fig. 3 shows an SEM image of $LaNiO_3$ nanotubes in a partially dissolved Al_2O_3 membrane with a typical diameter of 200 nm. The inset shows a top view of the membrane showing an excellent agreement between nanotube and pore diameters. The template method yields more homogeneous diameter distribution as compared to the hydrothermal synthesis. Dispersive X-ray energy (EDX) analysis on a spot over a nanotube confirms the presence of Ni and La, unlike areas not covered by NTs.

A powder X-ray diffraction (XRD) pattern of the NTs inside the alumina membrane is compared in Fig. 4 to the diffraction pattern of the bulk $LaNiO_3$ oxide prepared by thermal decomposition at 600 °C of the same precursor. The XRD patterns show characteristic reflections of the perovskite structure with a low fraction of segregated NiO (* indicates peaks due to NiO) associated to the slight excess in the Ni:La

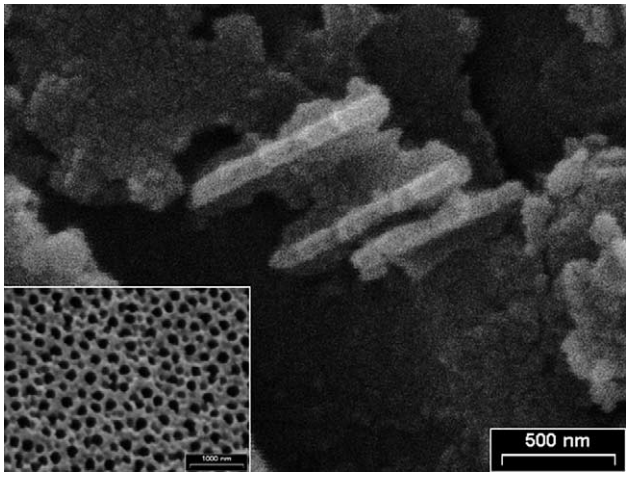

Fig. 3. Typical SEM micrograph of $LaNiO_3$ nanostructures grown in alumina template by thermal decomposition of $NH_4La[Ni(NO_2)_6]\cdot xH_2O$ at 600 °C. The inset shows a top view of the alumina template.

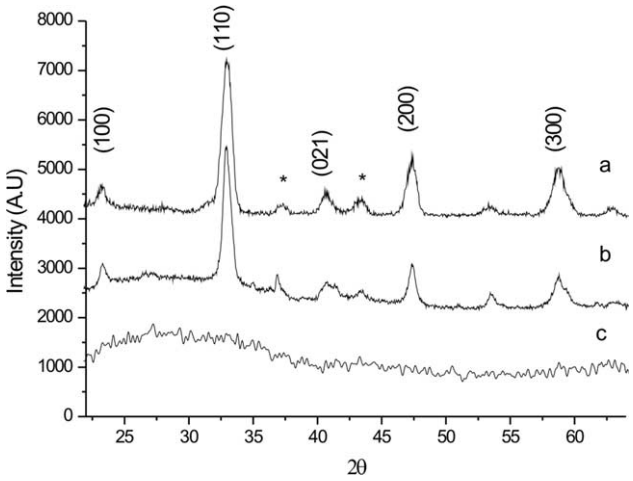

Fig. 4. XRD pattern of $LaNiO_3$ powder obtained at 600 °C (a); crushed alumina membrane containing $LaNiO_3$ nanotubes (b) and blank of crushed alumina template (c). Asterisks indicate peaks due to NiO.

ratio. However, it should be emphasized the lower NiO proportion with respect to higher temperature synthesis [20].

In Fig. 5, typical TEM images of template-free $LaNiO_3$ hollow nanostructures with internal separations can be seen with average diameters around 200 nm and a low size dispersion, ca. ±50 nm. The diameters are in close agreement with the alumina membrane nominal pore size (0.2 μm) and the SEM images in the inset of Fig. 3. To the best knowledge of the authors, these bamboo-like tubular nanostructures with internal separations have not been reported before for template-built NTs. It is supposed that these structures arise from de-wetting of the precursor solution on the hydrophilic alumina pore walls and also from the exhaust of gases during thermal decomposition.

An important observation in the TEM images is the very thin external walls of only 10–20 nm, with crystals randomly

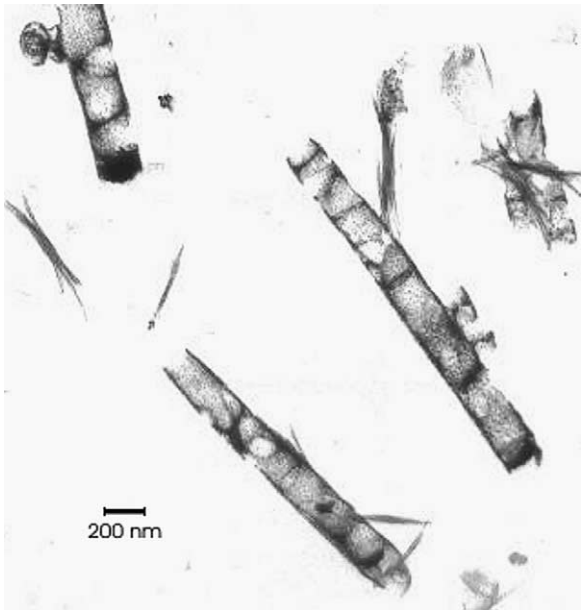

Fig. 5. TEM micrograph of $LaNiO_3$ hollow tubular nanostructures with bamboo-like internal partitions.

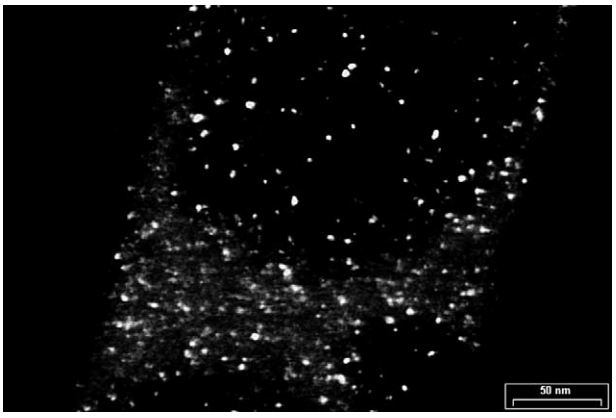

Fig. 6. TEM dark field micrograph of $LaNiO_3$ NTs showing small nanocrystals (3–5 nm) in the nanotube wall.

oriented and with typical 3–5 nm average length (dark field in Fig. 6). These are much smaller than previously reported nanosized $LaNiO_3$ crystals, ca. $\geq$12 nm [29].

The novel feature in these nanostructures is that only a few unit cells are contained in each 3–5 nm crystallite since $LaNiO_3$ has the rhombohedral distorted cubic perovskite structure [20,34–35] with unit cell parameters of 0.5456 and 1.3122 nm. This brings about the possibility to observe size confinement effects that would result in size dependent electronic and magnetic properties which are being investigated at present.

The $LaNiO_3$ tubular nanostructures reported in this communication resemble the metal nanoparticle-nanotubes described by Lahav and Rubinstein [36].

4. Conclusions

The combination of (i) a soluble inorganic Ni complex precursor with NO_2^- oxidant ligands with the appropriate La–Ni ratio and (ii) a porous template impregnated with the liquid solution of this precursor results in $LaNiO_3$ nanotubes upon relatively low temperature calcination, which has been characterized by SEM, TEM, DF-TEM and XRD. The as-prepared nanotubes show 200 nm in diameter and 10–20 nm walls comprised of very small crystals of about 3–5 nm. These results would not be possible by employing ceramic or sol–gel classical methods.

Acknowledgements

Financial support from CONICET and University of Buenos Aires is greatly appreciated. E.J.C., RDS and HET are research staff of CONICET (Argentina).

References

[1] L.-B. Kong, Solid State Commun. 133 (2005) 527–529.
[2] G.S. Wu, T. Xie, X.Y. Yuan, Y. Li, L. Yang, Y.H. Xiao, L.D. Zhang, Solid State Commun. 134 (2005) 485–489.
[3] X. Shen, A. Yuan, F. Wang, J. Hong, Z. Xu, Solid State Commun. 133 (2005) 19–22.
[4] P. Levy, A.G. Leyva, H.E. Troiani, R.D. Sanchez, Appl. Phys. Lett. 83 (2003) 5247–5249.
[5] J. Curiale, R.D. Sanchez, H.E. Troiani, H. Pastoriza, P. Levy, A.G. Leyva, Phys. B: Condens. Matter 354 (2004) 98–103.
[6] F.D. Morrison, Y. Luo, I. Szafraniak, V. Nagarajan, R.B. Wehrspohn, M. Steinhart, J.H. Wendorff, N.D. Zakharov, E.D. Mishina, K.A. Vorotilov, A.S. Sigov, S. Nakabayashi, M. Alexe, R. Ramesh, J.F. Scott, Rev. Adv. Mater. Sci. 4 (2003) 114.
[7] Y. Luo, I. Szafraniak, N.D. Zakharov, V. Nagarajan, M. Steinhart, R.B. Wehrspohna, J.H. Wendorff, R. Ramesh, M. Alexe, Appl. Phys. Lett. 83 (2005) 440.
[8] L. Zhao, M. Steinhart, M. Yosef, S.K. Lee, T. Geppert, E. Pippel, R. Scholz, U. Gösele, S. Schlecht, Chem. Mater. 17 (2005) 3.
[9] L. Huso, N. Mathur, Nature 427 (2004) 301.
[10] D. Zhu, H. Zhu, Y.H. Zhang, J. Phys.: Condens. Matter 14 (2002) L519–L524.
[11] J.J. Urban, L. Ouyang, M.H. Jo, D.S. Wang, H. Park, Nano Lett. 4 (2004) 1547–1550.
[12] J.B. Goodenough, J. Appl. Phys. 37 (1966) 1415–1422.
[13] R.D. Sanchez, M.T. Causa, J. Sereni, M. Vallet-Regi, M.J. Sayagues, J.M. Gonzalez-Calbet, J. Alloys Compd. 191 (1993) 287.
[14] J. Drennan, C.P. Tavares, B.C.H. Steele, Mater. Res. Bull. 17 (1982) 621–626.
[15] E. Calvo, J. Drennan, B.C.H. Steele, W.J. Albery, Proc. Electrochem. Soc. 84 (1984) 489.
[16] S.K. Tiwari, J.F. Koenig, G. Poillerat, P. Chartier, R.N. Singh, J. Appl. Electrochem. 28 (1998) 114–119.
[17] D.H. Bao, X. Yao, K. Shinozaki, N. Mizutani, J. Cryst. Growth 259 (2003) 352–357.
[18] D.H. Bao, N. Mizutani, X. Yao, L.Y. Zhang, Appl. Phys. Lett. 77 (2000) 1041–1043.
[19] T. Aytug, B.W. Kang, C. Cantoni, E.D. Specht, M. Paranthaman, A. Goyal, D.K. Christen, D.T. Verebelyi, J.Z. Wu, R.E. Ericson, C.L. Thomas, C.Y. Yang, S.E. Babcock, J. Mater. Res. 16 (2001) 2661–2669.
[20] A. Wold, B. Post, E. Banks, J. Am. Chem. Soc. 79 (1957) 4911.
[21] P.M. Raccah, J.B. Goodenough, Mater. Res. Bull. 8 (1973) 405.
[22] J. Takahashiet, J. Mater. Sci. 25 (1990) 1557.
[23] A.K. Norman, M.A. Morris, J. Mater. Process. Technol. 93 (1999) 91–96.
[24] M. Pechini, US Patent 3231328, 1966.
[25] A.D. Li, C.Z. Ge, P. Lu, N.B. Ming, Appl. Phys. Lett. 68 (1996) 1347–1349.
[26] H. Wang, Y.F. Zhu, P. Liu, W.Q. Yao, J. Mater. Sci. 38 (2003) 1939–1943.
[27] C.P. Tavares, Thermodynamic and Structural Relationships in the La–Ni–O System, Metallurgy and Materials Science, University of London, Imperial College, London, 1981.
[28] A. Bolibar, M. Insausti, L. Lorente, J.L. Pizarro, M.I. Arriortua, T. Rojo, J. Mater. Chem. 7 (1997) 2259–2264.
[29] H. Wang, Y.F. Zhu, P. Liu, W.Q. Yao, J. Mater. Sci. 38 (2003) 1939–1943.
[30] Z. Liang, A.S. Susha, A. Yu, F. Caruso, Adv. Mater. 15 (2003) 1849–1853.
[31] C.R. Martin, Science 226 (1994) 1961.
[32] M.A. Hitchman, D.L. Goodgame, Inorg. Chem. 3 (1964) 1389–1394.
[33] S. Takagi, Acta Cryst. B32 (1976) 2524.
[34] G. Demazeau, A. Marbeuf, M. Pouchard, P. Hagenmuller, J. Solid State Chem. 3 (1971) 582.
[35] J.M. Gonzalez-Calbet, M.J. Sayagués, M. Vallet-Regí, Solid State Ionics 32/33 (1989) 721–726.
[36] M. Lahav, T. Sehayek, A. Vaskevich, I. Rubinstein, Angew. Chem. Int. Ed. 42 (2003) 5575–5579.